Nuclear Instruments and Methods in Physics Research A 763 (2014) 184–189

Contents lists available at ScienceDirect

Nuclear Instruments and Methods in Physics Research A

journal homepage: www.elsevier.com/locate/nima

A novel source of MeV positron bunches driven by energetic protons for PAS application

Zongquan Tan [a,b,1], Wenzhen Xu [a,b], Yanfen Liu [a,b], Ran Xiao [a,b], Wei Kong [a,b], Bangjiao Ye [a,b,*]

[a] State Key Laboratory of Particle Detection and Electronics, University of Science and Technology of China, Hefei, Anhui 230026, PR China
[b] Department of Modern Physics, University of Science and Technology of China, Hefei, Anhui 230026, PR China

ARTICLE INFO

Article history:
Received 13 September 2013
Received in revised form
13 April 2014
Accepted 15 May 2014
Available online 11 June 2014

Keywords:
MeV positron bunches
Proton beam
CSNS
Fast chopper
PAS

ABSTRACT

This paper proposes a novel methodology of MeV positrons generation for PAS application. Feasibility of this proposal analyzed by G4Beamline and Transport have shown reasonable success. Using 2 Hz, 1.6 GeV, 100 ns and 1.5 μC/bunch proton bunches for bombarding a graphite target, about 100 ns e^+ bunches are generated. Quasi-monochromatic positrons in the range of 1–10 MeV included in these bunches have a flux of $>10^7$/s, peak brightness of 10^{14}/s. A magnetic-confinement beamline is utilized to transport the positrons and a "Fast Beam Chopper" is unprecedentedly extended to chop those relativistic bunches. The positron beam can be finally characterized by the energy range of 1–10 MeV and bunch width from one hundred ps up to 1 ns. Such ultrashort bunches can be useful in tomography-type positron annihilation spectroscopy (PAS) as well as other applications.

1. Introduction

PAS is a unique nondestructive method to investigate microscopic characteristic of materials. Its field of application has evolved over the last four decades from fundamental physics and chemistry to a phase in which PAS industrialization is becoming apparent [1]. Because of its sensitivity to changes in the concentration and arrangement of crystal lattice defects and insensitivity to macroscopic stress, PAS is highly desirable for describing damages and service-life-relevant aging processes in plant materials/components [2]. Nevertheless, the small penetration depth and requirement of specially prepared samples might limit its further evolution [3]. Positrons of variable energies in MeV range have shown their capacity for depth profiling of defects from micrometer to centimeter resolution [4]. They can even pass through a thin window before being implanted into a sample, which enables in-situ measurements with the sample under extreme conditions (e.g. high temperature, high pressure and high stress). Besides, with MeV positron beam, only single-sample pieces are required and restrictions for sample geometric shapes can be basically eliminated. Consequently, defects characterization of bulk materials/components in industrial environments is likely to be conducted.

Several types of MeV positron sources have been proposed, like β^+ emitters and large-scale facilities (nuclear reactors and linear accelerators). The β^+ emitters are routinely the main source for positron production, but they always encounter the bottleneck of low intensity. Appreciably higher intensity can be furnished in the large-scale facilities, however, a large area of converter–moderator section and the corresponding infrastructures limits their wide applications. Another set-up of the similar function is the photon-induced positron sources, like GiPS and PIPA [5,6]. But their gamma background is an especially serious problem, and because the incident gammas are not monoenergetic, the souce can not be used for tomography. Since large proton accelerators and, in particular, spallation neutron sources come into vogue [7], a novel positron source based on energetic protons can be expected. This type of source can always produce the highest positron intensity and widest continuous energy spectrum. The 1.6 GeV pulsed proton beam at China Spallation Neutron Source (CSNS) is illustrated schematically in Fig. 1 to drive the novel positron source. After being produced by protons impinging on a graphite target and captured by a quadrupole magnet triplet, more than 10^8/s positrons between 1 and 10 MeV are attainable. Subseqently, quasi-mono-energetic MeV positron bunches of high intensity are likely to be obtained just through an energy selector, e.g., 10^7/s for 3 MeV with 5 percent energy spread. Thus any moderator or linear accelerator for re-acceleration might not be indispensable, which should gain great attention in the research communities of energetic proton beam and MeV positron beam.

* Corresponding author at: State Key Laboratory of Particle Detection and Electronics, University of Science and Technology of China, Hefei, Anhui 230026, PR China
E-mail addresses: tqq1123@mail.ustc.edu.cn (Z. Tan), bjye@ustc.edu.cn (B. Ye).
[1] The first author.

http://dx.doi.org/10.1016/j.nima.2014.05.054
0168-9002/

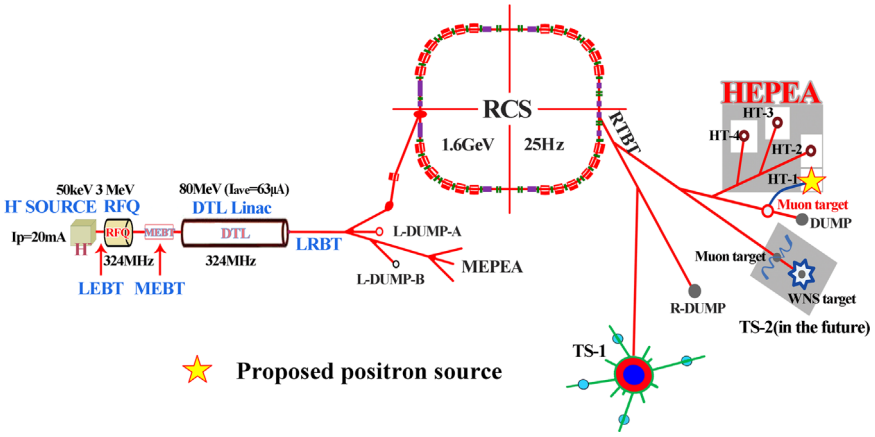

Fig. 1. The schematic of CSNS layout. A high energy proton experimental area (HEPEA) is arranged at CSNS and the position of proposed positron source is marked by a five-pointed star.

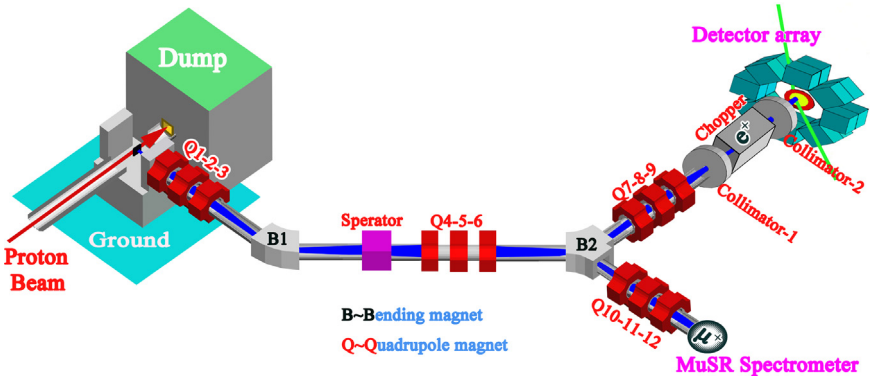

Fig. 2. The schematic drawing of pulsed MeV Positron Beam Transport (MPBT) with a detector-array at the end; It mainly includes the front end of surface-muon beamline (including an energy selector B1 and a particle separator) and a high-accuracy fast chopper with two collimators apart on both sides.

For PAS application, a conventional muon beam line is used to focus and transport positrons. A fast chopper is used to shorten the bunch width to within 1 ns. These ultrashort bunches are utilized for trigger signal in coincidence measurement, and gamma rays emitted from the sample, which are captured by detectors, are exploited for stop signal. PAS instruments would thus be available, like positron annihilation lifetime spectroscopy (PALS), positron emission tomography (PET), positron age-momentum correlation (AMOC) and so on.

2. Facility layout and design overview

CSNS is a large-scale accelerator facility consisting mainly of a H^- linac and a proton rapid cycling synchrotron (RCS). It is designed to accelerate proton pulses to 1.6 GeV at a repetition rate of 25 Hz, and to deliver a beam power of 120 kW in the first phase (500 kW in the second phase) [8]. 1 Hz proton pulses are extracted from RCS to HEPEA [9]. Each pulse contains two gaussian bunches in about 500 ns with the FWHM of 70 ns (Fig. 3).

The position of positron source is seen in Fig.1 and the overall layout of MPBT is illustrated schematically in Fig. 2. Using proton bunches for impinging on a graphite target, muon and positron bunches are generated of similar time structures [10]. Since the interchangeability between muon and positron bunches is to be implemented by a particle separator, muon beamline can be shared by positrons through periodically changing the working parameters of the beamline. It reasonably provides us a platform to certify the feasibility of our design. Furthermore, a μ^+–e^+ symbiont deserves our expectation. The main difference between muon and positron bunches is that the maximum width of the

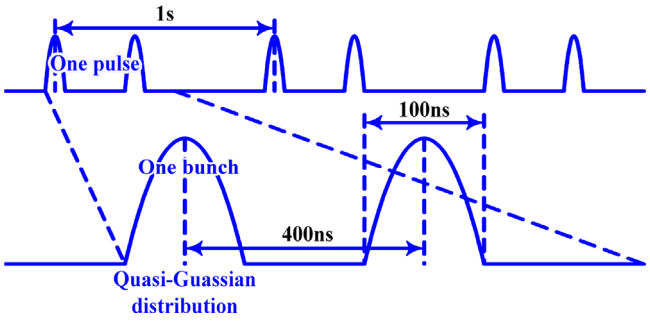

Fig. 3. The time structure of proton beam at HEPEA extracted from CSNS main proton beam.

latter should be additionally shortened to 1 ns, which is responsible for PAS application. A “Fast Chopper” driven by DC high voltage generator is proposed to meet this requirement. To our knowledge, it is the first attempt to find a proper chopper for MeV positron beam chopping. Compared with conventional PAS, another new concept of “Detector Array” should be considered. It means that, to achieve good detection efficiency, plenty of detectors are required to be assembled together as stop detectors, which form a large solid angle coverage around the sample. Their technical details will be discussed in the next chapter.

Innovations (like novel method of positron generation and first attempt of fast chopper and detector array in MeV-PAS) and advantages (like pulsed nature, adjustability of energy in MeV range and co-existence with muon beamline) can be apparently found in our design. Besides, many other superiorities will emerge

in PAS experiments: remarkably higher coincidence rate ~1 about 10–30 times higher than the conventional double-gamma coincidence (typically 0.04 in the case of plastic scintillator), appreciably lower time jitter (between chopper and sample), scarcely any restriction for sample geometric shapes, reduced systematic contribution from positron source and simplified data analysis.

3. Design of pulsed MeV positron beam facility

3.1. Positron generation mechanism

For positron generation, three fundamental sources can be commonly applied: isotope source, reactor core based source and accelerator-based source [11]. The mean energy of positrons in these sources is a few hundred keV. For this reason, they have to be decelerated in a moderator typically made of tungsten and subsequently accelerated to expected energies. A new method for positron generation is proposed at CSNS that positrons are produced by thermal protons being captured in a graphite target. Compared with its counterparts (e.g. an accelerated 1.5 or 3 MeV deuteron beam hitting a graphite target to create a β^+ emitter via $^{12}C(d,n)^{13}N$ reaction [12,13]), more modes of positron generation are triggered at 1.6 GeV and they can be divided into two stages: (1) "evaporation" or "continuous" stage: direct decay of β^+ emitters (e.g. ^{12}N, ^{13}N, ^{14}C, ^{11}C [14]), indirect decay of π^+ mesons $\pi^+ \rightarrow \mu^+ \overset{2.2\,\mu s}{\rightarrow} e^+$ and de-excitation of nuclear levels; (2) "cascade" or "pulsed" stage: pair production through bremsstrahlung of proton or other secondary charged particles (e.g. e^+, e^-,π^+,$\pi-$) and decay of π^0 mesons ($\pi^0 \overset{8.4\times10^{-17}\,s}{\rightarrow} \gamma \rightarrow e^+e^-$). Prompt positrons are produced in the pulsed stage. The temporal profile of proton pulse is thus fully transferred to positron beam (Fig. 4) and a continuous positron spectrum from 0 up to several hundred MeV is obtained (Fig. 5). In this stage, positrons in the range of 0–10 MeV come mainly from the bremsstrahlung of charged particles [15] and the corresponding cross section approximately varies with $\sim E \ln E$ [16], where E is the incident kinetic energy of protons. Thus, the energy of 1.6 GeV possesses a huge advantage in the yield of positrons. Positrons from the pulsed stage have accordingly had a strong impression on us and they are to be used for PAS experiment. Details will be expounded emphatically in the subsequent sections.

Graphite, a low-Z material, has been selected as the target with length, width and height all of 60 mm [17]. The physical processes of positron production in the target and the capture by quadrupole magnets are simulated by G4beamline code. The time structure of positrons collected in the first quadrupole triplet Q1-2-3 is presented in Fig. 4. Positrons produced in the pulsed stage are taken as a Gaussian profile and positrons from the continuous stage are shaped as an exponential distribution. These results further demonstrate the generation modes of positrons described above. Counts of positrons

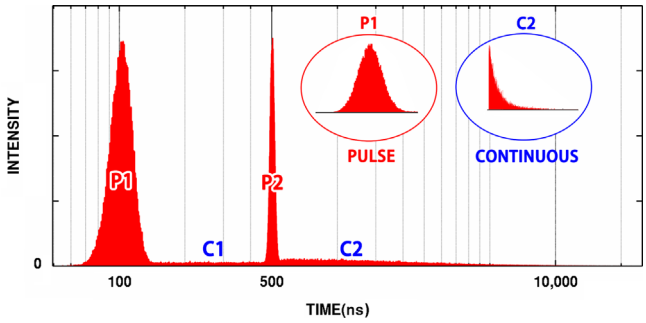

Fig. 4. The full time spectrum of positrons obtained in Q1 from G4beamline by taking logarithm of time-coordinate; the upper-right subgraphs are enlarged drawings of the pulse part P1 and the continuous part C2.

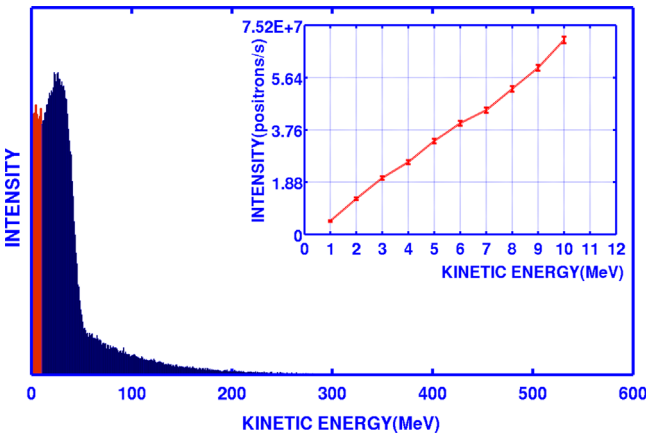

Fig. 5. The full energy spectrum of positrons collected in the first quadrupole magnet triplet, with the upper-right graph of positron yield corresponding to integral energies from 1 to 10 MeV (energy spread of 5 percent) and their corresponding error bars (the vertical bars).

over 10^7/s are obtained at any energy between 1 and 10 MeV with 5 percent energy spread in Q1 (Fig. 5). Thus, it is possible to directly obtain intense quasi-mono-energetic MeV positrons independent of any moderator or re-accelerator. Due to the complexity of measuring process, no facility has directly measured the relativistic positrons coming out from the target. These simulation results will be taken as a basis for designing transport line.

3.2. Beam transport line

A conventional beamline is under construction at CSNS to supply monochromatic surface-muons for Muon Spin Rotation, Relaxation and Resonance experiments [18]. The schematic drawing of this beamline is shown in Fig. 2. Positrons emerging from the target surface are collected and focused by Q1-2-3 (collection at 90° from proton beam direction). To acquire quasi-homochromatic positrons, the focused beam is bent by 45° through B1, which can be adjusted to accept positrons within several percent energy spread, e.g., 3 MeV positrons (5 percent energy spread) are extracted and are to be applied in the next simulation and calculation. Subsequently, "impure" particles, mainly positive muons, are decontaminated in a separator. To establish proper time structure, beam size and angular divergence before physics experiments, a chopping system is required [19]. It contains a dual-planar chopper to shorten bunch width, and two collimators arranged on both sides of the chopper to ensure proper beam spot size and angular divergence.

Beam dynamics simulation (envelope calculation, phase space matching, multi-particle tracking) is performed by Transport. It aims to find an optimum position for chopper installing. It is a nontrivial optimization task with the following main objectives: to minimize transverse halo at the exit of chopper, to minimize chopper voltage and to make beamline more compact. The simulation has been done by using the distribution (result from G4beamline) in Q1 as the initial input. It allows the analysis of emittance increasement and the halo development generated in MEPT. The envelope of 3 MeV positrons in transverse plane is exhibited in Fig. 6. The beam double-waist (LV5), about 20 mm extent in transverse plane and 2 m away from SQ9, indicates the chopper location.

3.3. Beam chopping system

3.3.1. Design of fast chopper

It is still vacant presently to use a chopper to chop the relativistic positron beam. In our case, off-peak component of

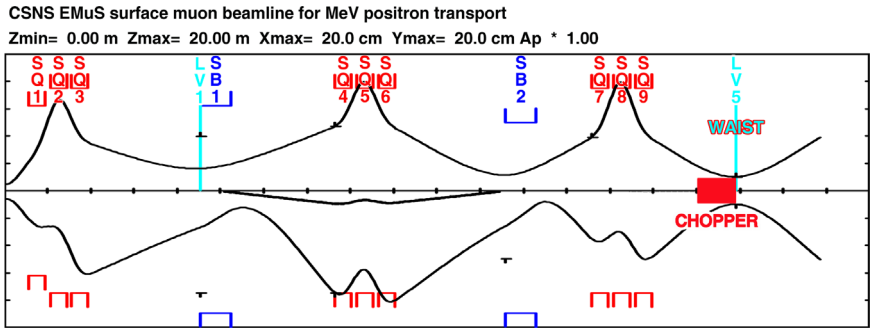

Fig. 6. The beam envelope of 3 MeV positrons in MPBT with the chopper switched off, a double waist (LV5) is found at about 2 m after Q9.

bunches is to be removed while 1 ns or less is to be remained. This puts a challenge on chopping technics, meanwhile, it is the key to the feasibility of the PAS experiments. The transmission-line type of dual-planar chopper supported by DC high-voltage generator can be a candidate for its superiority in high voltage and system rise time. This type of chopper has been developed for the chopping of medium energy (several MeV) H^- beam in ESS-RAL, LANL-SNS, JAERI, CERN-SPL etc. over ten years [20]. Quasi-trapezoidal bipolar high-voltage pulses seen in Fig. 7 are accordingly utilized to deliver transverse radio-frequency (RF) electric field [21].

To establish priority of all parameters and specifications, the system rise time is preferential to be considered, for it relates directly to the bunch width at output. The system rise time is approximately provided by [22]:

$$t_R = \sqrt{t_G^2 + t_S^2} \tag{1}$$

where t_G is the generator rise time and t_S is the structure rise time. The state-of-art is identified that the lower limit of t_G is 2 ns or slightly less at the high voltage of 1.5 kV [23]. Since deflectors are likely to be driven at opposite polarities, a total effective voltage of 3 kV is available. For the designing of chopper structure, the reasonable goal should be to add as few t_S as possible to overall system rise time t_R. The former is given by:

$$t_S = \tau \times \left(1 \pm \frac{\beta_b}{\beta_\omega}\right), \tau = \frac{L}{\beta_b c} \tag{2}$$

where β_b, β_ω and L are respectively the beam velocity, the effective wave velocity and the deflector length. Positive sign corresponds to the opposite direction of positron beam and high voltage wave propagation, while sign reverses in the same direction. With the choice of the transmission-line configuration seen in Fig. 8 or other counterparts with delay lines [24], electric field can travel almost simultaneously with particles through (3 MeV positrons with a relativistic velocity ~0.989 c). Therefore, the structure rise time is to be reduced or better neglected.

3.3.2. Calculation

After passing through the collimator installed before the chopper, a count of 2×10^5e+/100 ns, or average 0.4 μA current in one bunch, is obtained from the transport. Space-charge effects in this current can be neglected and "single particle model" (SPM) is likely to be applicable during calculation. It means a superposition of non-interacting particles after being separately calculated. Setting the electrode gap of the chopper to be equal to 20 mm (the maximum possible size of beam spot at exit), positrons after being collimated by the preposed collimator can entirely pass through the deflectors and postposed collimator when there is no electrical deflection. The SPM is thus to be

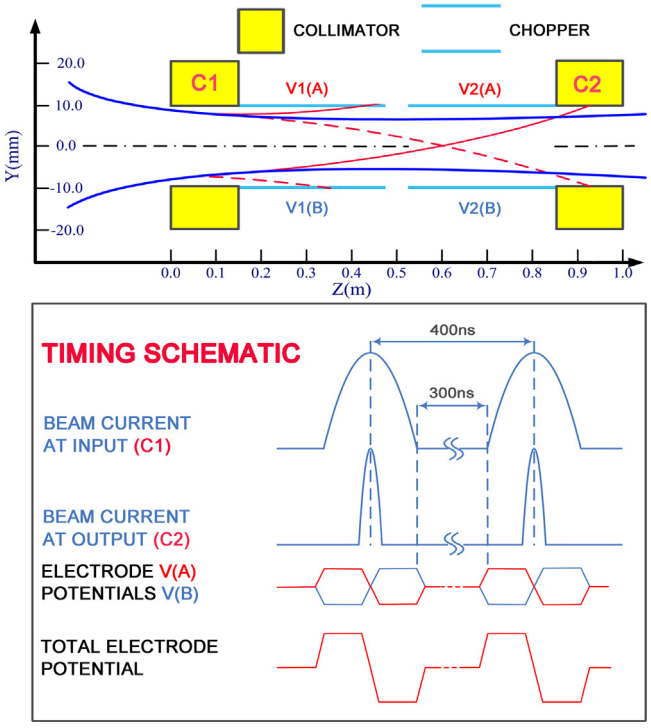

Fig. 7. The structure of "Fast Chopper" with the tandem distribution of two sub-choppers and the corresponding timing schematic.

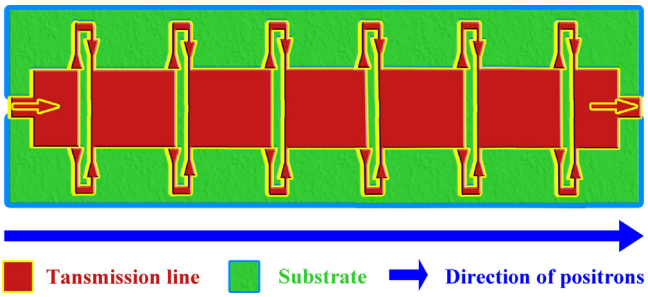

Fig. 8. A typical configuration of transmission-line deflectors: several short strip lines connected by delay lines.

further characterized by zero angular divergence. Provided that there is a high coverage factor (~1), there is a very low attenuation of RF electric field and perfect synchronization between the traveling-wave and positron beam. Transverse displacement Δy of

the relativistic positrons can be estimated as:

$$\Delta y = \frac{\varepsilon_0}{qE}\left(ch\frac{qE}{P_0 c}L - 1\right), \quad E = V/d, \quad \varepsilon_0 = m_0c^2 + V_T \tag{3}$$

where q is the electronic charge, m_0 is the rest mass, L is the effective electrode length, V is the deflecting potential, d is the electrode gap and P_0, ε_0, V_T are respectively the initial momentum, the total energy and the kinetic energy of the incident positrons.

A proper set of parameters seen in Table1 is selected as been routinely used, internationally [20]. A deflection distance of 20 mm is required to guarantee the unwanted partial of bunches to be pneumatically removed. A minimum of high voltage on the single deflector should be set to 0.2 kV. After calculation, an optimum time resolution ~150 ps is obtained. However, a combination of 500 ps and $3.4\times10^3 e^+/s$ (bunch FWHM and count rate) at 0.5 kV is to be preferred (Fig. 9), for this intensity is enough for normal experiments and that, furthermore, relatively low voltage can relieve rigorous requirements for the chopping technics. It is only the result of 3 MeV positrons presented above. However, energy range can be expanded actually to around 10 MeV and the corresponding time resolution can still retain within 1 ns.

3.4. Detector spectrometer

In coincidence measurements, high-voltage pulses and annihilation gammas are respectively taken for the start signal and stop signal. In our spectrometer, 64 prepositive and 64 postpositive detectors are symmetrically installed to detect 0.511 MeV annihilation gammas, like the Dai Omega-Kai built at at J-Parc/Muse, which is furnished with 128 counters (10 percent of all solid angle) to handle 2×10^4 μ^+/spill (typically 100 ns width) [25]. This design aims at a sufficient count rate, an excellent peak-to-background ratio [26] and an unique platform for AMOC. After penetration into the sample, positrons annihilate with the individual lifetime τ_i in different types of electron holes and their count rates exponentially vary with the time t: $I_i(t) = I_i e^{-(t/\tau_i)}$, the loss of gamma events in detectors can thus be given as a probability [26]:

$$P = \int_0^{+\infty} P(t)dt = \int_0^{+\infty} \sum_{i=1}^{n} P_i(t)dt = \frac{dI}{2m}; \quad Pi(t) \simeq \frac{dIi(t)}{2\tau im} \tag{4}$$

where m is the number of detectors and $I = 10\%I_0 = 340e^+/s = 170e^+$/bunch is the gamma count rate detected by the spectrometer. Basically, two factors account for the count loss: one is the time resolution of the detector system d_1 (typically about 200 ps for 0.511 MeV gamma detection), within which two adjacent signals will be piled up; the other one is the deadtime of the electronic system d_2 (typically about 20 ns), during which gammas will be lost after one gamma being detected. According to the formula (4), the count loss due to the latter factor is obviously predominant. However, in our case, positron bunch width (500 ps) is much less than d_2, which means that one detector can only detect one gamma per bunch, or that the final count rate is basically determined by the number of detectors: $64e^+$/bunch or $128e^+/s$. The corresponding bunch FWHM can be reduced to below 200 ps. Normal PAS instruments like PALS, AMOC, etc., with this specified detector array distribution would be prevalent and another apparatus, PET, for 3D imaging and assaying of defects in thick materials should also be candidates.

Table 1
Key parameters for the fast chopper.

Parameters	Units	Values
High voltage	kV	0.2–1.5 kV
Transition time	ns	2
Pulse duration	ns	50
Electrode length	mm	350+350 (tandem)
Electrode gap	mm	20

4. Summary and prospects

In this study, we proposed a novel positron source driven by the 1.6 GeV pulsed proton beam at CSNS. A conventional muon transport line is utilized to capture, focus and transport MeV positrons. Through a fast chopper of the internationally identified parameters, quasi-homochromatic MeV positron bunches with a count of 10^3–$10^4 e^+/s$ and time resolution of several hundred ps can be eventually obtained, thus presenting a successful proof of feasibility.

Furthermore, the final count rate can still be improved mainly from the following three aspects: (1) the positron bunch frequency: it is directly proportion to the final count rate, 2 Hz in our case reserves a large rising space, (2) the number of positron detectors: higher-segmented positron-detection technologies are actually mature, for example, a 606-counter positron-detection system is under construction at RIKEN-RAL [27]. (3) The positron beam intensity: employing a more efficient capture system, an appreciably higher intensity is promising to be expected, e.g., 1000 times higher capture efficiency than the conventional collection by

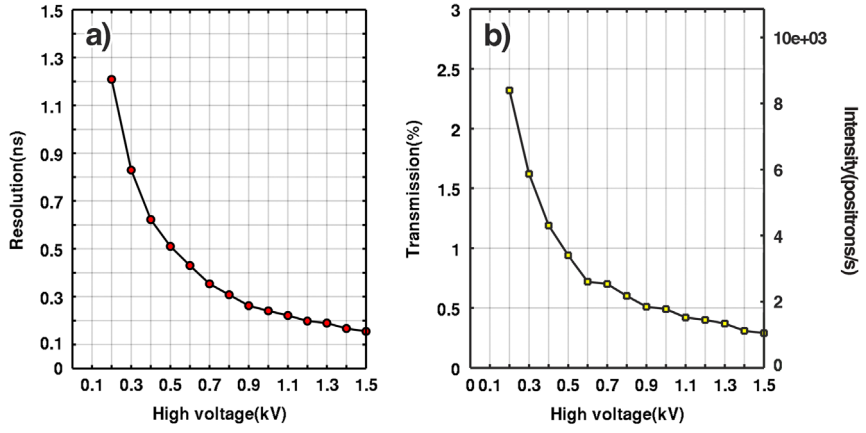

Fig. 9. The high voltage of single deflector versus (a) the time resolution arising from bunch width (i.e. bunch FWHM), and (b) the positron transmission rate (the left vertical coordinate) and beam intensity at the exit of chopper (the right vertical coordinate).

quadrupole magnets has already been implemented in MuSIC (Japan) [28] by using superconducting solenoid magnets.

Acknowledgment

Financial support for this research was provided by National Natural Science Foundation of China (no. 11075154). We wish to thank Ran An, Hong Yan, Shancai Zhang, Ji Li, Ruixuan Huang, Shijuan Huang and Shengqun Tong for their useful discussion and suggestion.

References

[1] P. Coleman, Nuclear Instruments and Methods in Physics Research Section B: Beam Interactions with Materials and Atoms 192 (2002) 83.
[2] G. Dobmann, N. Meyendorf, E. Schneider, Nuclear Engineering and Design 171 (1997) 95.
[3] G. Sposito, C. Ward, P. Cawley, P. Nagy, C. Scruby, NDT&E International 43 (2010) 555.
[4] R. Batra, M. Sehgal, Physical Review B 23 (1981) 4448.
[5] M. Butterling, W. Anwand, T.E. Cowan, A. Hartmann, M. Jungmann, R. Krause-Rehberg, A. Krille, A. Wagner, Nuclear Instruments and Methods in Physics Research Section B: Beam Interactions with Materials and Atoms 269 (2011) 2623.
[6] P. Pujari, K. Sudarshan, R. Tripathi, D. Dutta, P. Maheshwari, S. Sharma, D. Srivastava, R. Krause-Rehberg, M. Butterling, W. Anwand, et al., Nuclear Instruments and Methods in Physics Research Section B: Beam Interactions with Materials and Atoms 270 (2012) 128.
[7] I. Gardner, et al., A review of spallation neutron source accelerators, in: Proceedings of EPAC, 98, 1998.
[8] J. Wei, H. Chen, Y. Chen, Y. Chen, Y. Chi, C. Deng, H. Dong, L. Dong, S. Fang, J. Feng, et al., Detectors and Associated Equipment 600 (2009) 10.
[9] W. Sheng, F. Shou-Xian, F. Shi-Nian, L. Wei-Bin, O. Hua-Fu, Q. Qing, T. Jing-Yu, W. Jie, Chinese Physics C 33 (2009) 1.
[10] H. Jing, C. Meng, J. Tang, B. Ye, J. Sun, Detectors and Associated Equipment 684 (2012) 109.
[11] S. Golge, B. Vlahovic, et al., Review of low-energy positron beam facilities (2012).
[12] D. Cassidy, K. Canter, R. Shefer, R. Klinkowstein, B. Hughey, Nuclear Instruments and Methods in Physics Research Section B: Beam Interactions with Materials and Atoms 195 (2002) 442.
[13] A. Hunt, L. Pilant, D. Cassidy, R. Tjossem, M. Shurtli, M. Weber, K. Lynn, Applied Surface Science 194 (2002) 296.
[14] B. Kozlovsky, R. Lingenfelter, R. Ramaty, The Astrophysical Journal 316 (1987) 801.
[15] R. Ramaty, R. Murphy, Space Science Reviews 45 (1987) 213.
[16] D. URGA, Electron–positron pair production in collision of virtual photons and pair conversion of virtual bremsstrahlung photon (2007).
[17] Y. Liu, W. Xu, Z. Tan, Y. Liang, W. Kong, B. Ye, Mechanica & Astronomica 42 (2012) 1204.
[18] X. Wenzhen, L. Yanfen, Y. Bangjiao, Plasma Science and Technology 14 (2012) 469.
[19] M. Maekawa, M. Kondo, S. Okada, A. Kawasuso, H. Itoh, Radiation Physics and Chemistry 60 (2001) 525.
[20] F. Caspers, Technical Report, 2004.
[21] M.A. Clarke-Gayther, A fast chopper for the ESS 2.5 MeV beam transport line, in: Proceedings of the 8th European Particle Accelerator Conference, EPAC, 2, 2002.
[22] T. Kroyer, F. Caspers, E. Mahner, The CERN S.P.L. Chopper Structure. A Status Report, Technical Report, 2007.
[23] M. Clarke-Gayther, The development of a fast beam chopper for next generation high power proton drivers, IPAC2010, Kyoto, May, (2010).
[24] A. Aleksandrov, C. Deibele, T. Roseberry, New design of the sns mebt chopper deector, in: Particle Accelerator Conference, 2007. PAC. IEEE, IEEE, 2007, pp. 1817–1819.
[25] H. Tanaka, K. Nagamine, H. Miyadera, K. Shimomura, Y. Ikedo, K. Nishiyama, K. Ishida, Detectors and Associated Equipment 554 (2005) 201.
[26] R. Kadono, Y. Miyake, Reports on Progress in Physics 75 (2012) 026302.
[27] D. Tomono, T. Kawamata, Y. Hirayama, M. Iwasaki, I. Watanabe, K. Ishida, T. Matsuzaki, Progress in development of new sr spectrometer at riken-ral, in: Journal of Physics: Conference Series, volume 225, IOP Publishing, 2010, p. 012056.
[28] M. Yoshida, M. Fukuda, K. Hatanaka, Y. Kuno, T. Ogitsu, A. Sato, A. Yamamoto, IEEE Transactions on Applied Superconductivity 21 (2011) 1752.